

# One- and two-dimensional Bose-Einstein correlations in deep inelastic scattering at HERA

ZEUS Collaboration

## Abstract

Measurements of Bose-Einstein correlations in one and two dimensions are presented for deep inelastic  $ep$  scattering measured with the ZEUS detector at HERA using an integrated luminosity of  $82.6 \text{ pb}^{-1}$ . The two-particle correlation functions are independent of the virtuality of the exchanged photon,  $Q^2$ . The two-dimensional shape of the source was investigated in the longitudinally co-moving system for both the transverse and longitudinal components of the momentum difference with respect to the direction of the hadronic centre-of-mass system. A significant difference between the transverse and the longitudinal dimensions of the source is observed.



# 1 Introduction

For a pair of identical bosons, the quantum mechanical wave-function has to be symmetric under particle exchange. As a consequence, interference effects are expected between identical bosons emitted close to one another in phase space. These effects alter the two-particle density at small phase-space separations and lead to Bose-Einstein (BE) correlations, which were first observed by Goldhaber et al. [1] for like-charged hadrons in  $p\bar{p}$  annihilation.

The shape of the BE correlations in relative momentum space is related to the spatial dimensions of the production source. Therefore, studies of the BE effect may lead to a better understanding of the space-time structure of the source of the identical bosons. In deep inelastic scattering (DIS), a reduction of the correlations between identical particles should be observed with increasing virtuality of the exchanged photon,  $Q^2 = -q^2 = -(k - k')^2$  ( $k$  and  $k'$  denote the four-momenta of the initial- and final-state leptons, respectively), since the transverse size of the virtual photon decreases with increasing  $Q^2$ . Alternatively, the BE effect can be explained in the framework of the Lund fragmentation model [2, 3]. In this case, no sensitivity of this effect to the scale  $Q^2$  is expected, since the BE correlations between two identical pions is a measure of the string tension.

This paper investigates the BE correlations in one- and two-dimensions in neutral current  $e^+p$  DIS, focusing on studies of a dependence of the BE interference on  $Q^2$ . The BE correlations in one dimension are measured with a much higher precision than were previously done in  $ep$  collisions [4], and over a wide kinematic range from  $Q^2 \sim 0.1 \text{ GeV}^2$  to  $\simeq 5000 \text{ GeV}^2$ . Furthermore, for the first time in DIS, the correlations were studied in the longitudinal and transverse directions in order to probe the shape of the pion source.

## 2 Definition of the measured quantities

Bose-Einstein correlations are usually parameterised using a Gaussian expression for the normalised two-particle density [5]:

$$R(Q_{12}) = \alpha (1 + \beta Q_{12}) (1 + \lambda e^{-r^2 Q_{12}^2}), \quad (1)$$

where  $Q_{12} \equiv \sqrt{-(p_1 - p_2)^2} = \sqrt{M^2 - 4m_{boson}^2}$  is the Lorenz-invariant momentum difference between the two bosons, which is related to the invariant mass  $M$  of the two particles with four-momenta  $p_1$  and  $p_2$  and masses  $m_{boson}$ . The parameter  $\lambda$  is a measure of the degree of coherence, i.e. the fraction of pairs of identical particles that appear to interfere, while  $r$  is the radius of the production volume. The parameter  $\beta$  is used to take into account long-distance non-BE correlations.

To calculate  $R(Q_{12})$ , the inclusive two-particle density  $\rho$  was defined as  $\rho = (1/N_{\text{ev}})dn_{\text{pairs}}/dQ_{12}$ , where  $n_{\text{pairs}}$  is the number of particle pairs and  $N_{\text{ev}}$  is the number of events. The densities were calculated for like-charged particle combinations ( $\rho(\pm, \pm)$ ) and for unlike-charged combinations ( $\rho(+, -)$ ), and the ratio computed as  $\xi = \rho(\pm, \pm)/\rho(+, -)$ . This technique helps to remove correlations due to the topology and global properties of DIS events contributing to  $\rho(\pm, \pm)$ . The quantity  $\xi$  contains additional short-range correlations, due to resonance decays (mainly contributing to  $\rho(+, -)$ ), which should also be removed. In order to reduce such non-BE effects, a Monte Carlo sample without the effect was used to calculate the  $\xi^{\text{MC,noBE}}$ , and then non-Bose-Einstein effects were removed by use of the double ratio,  $R(Q_{12}) = \xi^{\text{data}}/\xi^{\text{MC,noBE}}$ .

The shape of the correlation function can also be studied in the transverse and longitudinal directions. For this, the longitudinally co-moving system (LCMS) [6] is often used, since it has a convenient interpretation. For  $ep$  collisions, the LCMS can be defined for each pair of particles with momenta  $\mathbf{p}_1$  and  $\mathbf{p}_2$ , as the system in which the sum of the two momenta,  $\mathbf{p}_1 + \mathbf{p}_2$ , is perpendicular to the  $\gamma^*p$  axis. The three-momentum difference,  $\mathbf{Q} = (\mathbf{p}_2 - \mathbf{p}_1)$ , can be decomposed in the LCMS into transverse,  $Q_T$ , and longitudinal,  $Q_L$ , components. The longitudinal direction is aligned with the direction of motion of the initial parton, therefore, in the string model, the system itself is the local rest frame of a string. The BE effect can be parameterised using the two-dimensional function:

$$R(Q_T, Q_L) = \alpha (1 + \beta_t Q_T + \beta_l Q_L) (1 + \lambda e^{-r_T^2 Q_T^2 - r_L^2 Q_L^2}), \quad (2)$$

where  $r_T$  and  $r_L$  reflect the transverse and longitudinal extent of the boson source. The measurements were done using the same procedure as that described for the one-dimensional study.

### 3 Experimental setup

ZEUS is a multipurpose detector described in detail elsewhere [7]. Of particular importance in the present study are the central tracking detector, the uranium-scintillator calorimeter and the Beam Pipe Calorimeter. The central tracking detector (CTD) [8] is a cylindrical drift chamber with nine super-layers covering the polar-angle<sup>1</sup> region  $15^\circ < \theta < 164^\circ$  and the radial range 18.2 – 79.4 cm. Each super-layer consists of eight

---

<sup>1</sup> The ZEUS coordinate system is a right-handed Cartesian system, with the  $Z$  axis pointing in the proton beam direction, referred to as the “forward direction”, and the  $X$  axis pointing left towards the centre of HERA. The coordinate origin is at the nominal interaction point. The pseudorapidity is defined as  $\eta = -\ln(\tan \frac{\theta}{2})$ , where the polar angle,  $\theta$ , is measured with respect to the proton beam direction.

sense-wire layers. The transverse-momentum resolution for charged tracks traversing all CTD layers is  $\sigma(p_T)/p_T = 0.0058p_T \oplus 0.0065 \oplus 0.0014/p_T$ , with  $p_T$  in GeV.

The CTD is surrounded by the uranium-scintillator calorimeter, CAL [9], which is divided into three parts: forward, barrel and rear. The calorimeter is longitudinally segmented into electromagnetic and hadronic sections. The smallest subdivision of the CAL is called a cell. The energy resolution of the calorimeter under test-beam conditions is  $\sigma_E/E = 0.18/\sqrt{E}$  for electrons and  $\sigma_E/E = 0.35/\sqrt{E}$  for hadrons (with  $E$  in GeV).

The Beam Pipe Calorimeter (BPC) [10] was installed 294 cm from the interaction point in order to enhance the acceptance of the ZEUS detector for low- $Q^2$  events. The BPC is a tungsten-scintillator sampling calorimeter with the front face located at  $Z = -293.7$  cm, the center at  $Y = 0.0$  cm, and the inner edge of the active area at  $X = 4.4$  cm, as close as possible to the rear beam pipe. The relative energy resolution as determined in test-beam measurements with 1–6 GeV electrons is  $\sigma_E/E = 17\%/\sqrt{E(\text{GeV})}$ .

## 4 Data sample

Two data samples were used for the present analysis. The data for medium and high- $Q^2$  events were taken during the 1998-2000 period, corresponding to an integrated luminosity of  $82.6 \pm 1.2 \text{ pb}^{-1}$ . The positron or electron beam energy was 27.5 GeV and the proton beam energy was 920 GeV. The second sample was for low- $Q^2$  events taken with the BPC. This sample corresponds to  $3.9 \text{ pb}^{-1}$  of the data taken during 1997, when the proton energy was 820 GeV.

The kinematic variables,  $Q^2$  and  $x$ , were reconstructed by the following methods:

- the electron method (this method is denoted by the subscript  $e$ ) uses measurements of the energy and angle of the scattered positron;
- the double angle (DA) method [11] relies on the angles of the scattered positron and of the hadronic energy flow;
- the Jacquet-Blondel (JB) method [12] is based entirely on measurements of the hadronic system.

The scattered-positron candidate for the medium and high- $Q^2$  events was identified from the pattern of energy deposits in the CAL [13]. This data sample contains the following DIS requirements:

- $E_{e'} \geq 10 \text{ GeV}$ , where  $E_{e'}$  is the corrected energy of the scattered lepton measured in the CAL;

- $40 \leq \delta \leq 60$  GeV, where  $\delta = \sum E_i(1 - \cos\theta_i)$ ,  $E_i$  is the energy of the  $i$ th calorimeter cell,  $\theta_i$  is its polar angle with respect to the beam axis and the sum runs over all cells;
- $y_e \leq 0.95$  and  $y_{\text{JB}} \geq 0.04$ ;
- a primary vertex position, determined from the tracks fitted to the vertex, in the range  $|Z_{\text{vertex}}| < 50$  cm;
- the impact point  $(X, Y)$  of the scattered positron in the calorimeter must be within a radius  $\sqrt{X^2 + Y^2} > 36$  cm.

Using these requirements, two data samples were selected:  $25 < Q_{DA}^2 < 40$  GeV<sup>2</sup> and  $Q_{DA}^2 \geq 110$  GeV<sup>2</sup>.

The low- $Q^2$  events, selected in the region  $0.1 < Q_e^2 < 1.0$  GeV<sup>2</sup>, were reconstructed with the BPC. The scattered positron was required to have an energy of at least 7 GeV for events reconstructed with the electron method. The positron position at the BPC front face had to lie within the fiducial area,  $5.2 < X < 9.3$  cm and  $-2.3 < Y < 2.8$  cm, yielding an angular acceptance of  $18 < \theta_e < 32$  mrad. In order to limit migrations from low  $y$ , a cut  $y_{\text{JB}} > 0.06$  was applied. Other cuts are identical to those used for the analysis of the high  $Q^2$  events (with the exclusion of the impact-point cut).

The analyses are based on the CTD tracks assigned to the primary event vertex. No particle identification is used. Tracks are required to pass through at least three CTD superlayers and have transverse momentum  $p_T^{\text{lab}} > 150$  MeV.

To ensure that the two particles are resolved, the angle between two tracks should not be smaller than two degrees [14]. Therefore, the region with  $Q_{12} < 0.05$  GeV was excluded from the analysis, since in this case a typical separation between two tracks is two degrees.

The measured correlation functions,  $R(Q_{12})$  and  $R(Q_T, Q_L)$ , were corrected for the detector effects using a bin-by-bin procedure. Correction factors were calculated as the ratios of the distributions at the generator level of a Monte Carlo sample to those at the reconstructed level. The corrections are close to unity in all cases, since some detector effects cancel in the ratios of the two-particle densities. The average  $Q^2$  values were also corrected.

## 5 Event simulations and systematic uncertainties

The Monte Carlo (MC) events were generated with the ARIADNE 4.07 model [15]. The model employs the PYTHIA/JETSET program [16], which is based on the Lund string model [17]. The BE effect, which is treated as a final state interaction by re-shuffling hadron momenta according to a chosen parameterisation, is available as an option in

these simulations. The two-particle densities for small  $Q_{12}$  are significantly better described by the ARIADNE model with the BE correlations, rather than without the BE effect<sup>2</sup>. Therefore, the BE correlations were included in the simulation for the acceptance calculations. The effect was parametrised by a Gaussian function with the H1 default parameters [4].

For the acceptance calculations, ARIADNE was interfaced with HERACLES 4.5.2 [18] using the DJANGO program [19] in order to incorporate first-order electroweak corrections. The generated events were then passed through a full simulation of the detector using GEANT 3.13 [20] and processed with the same reconstruction program as used for the data. The detector-level MC samples were then selected in the same way as the data.

The systematic uncertainties on the measured cross sections were estimated by varying the event-selection cuts, track quality cuts and changing the fit regions. The overall systematic uncertainty was determined by adding the above uncertainties in quadrature.

Identically charged particles are subject to the Coulomb repulsion, which is not simulated by MC models. As a check, the Bose-Einstein correlation function was corrected in the data using the Gamow factor [21]. After correcting for the Coulomb effect, the size of the BE radius slightly increases, but it is still within the statistical and systematic errors.

## 6 Results

### 6.1 One-dimensional study

Figure 1 shows the measured  $R(Q_{12})$  together with the fit to Eq. (1). The regions affected by imperfections in the simulations of  $K_s^0$  and  $\rho^0$  decays were excluded from the fit. The extracted parameters for  $Q^2 > 110 \text{ GeV}^2$  are

$$\begin{aligned} r &= 0.671 \pm 0.016(\text{stat.})_{-0.032}^{+0.030} (\text{syst.}) \text{ fm}, \\ \lambda &= 0.431 \pm 0.012(\text{stat.})_{-0.130}^{+0.042} (\text{syst.}). \end{aligned}$$

Figure 2 shows that the obtained BE parameters are in good agreement with the H1 values for  $6 < Q^2 < 100 \text{ GeV}^2$  [4]:  $r = 0.68 \pm 0.04_{-0.05}^{+0.02} \text{ fm}$  and  $\lambda = 0.52 \pm 0.03_{-0.21}^{+0.19}$  (the data point is shown for the mean value of  $Q^2$  in the interval  $6 < Q^2 < 100$ ). Furthermore, the measured effect also agrees with the LEP1-LEP2 measurements [22], when the Gaussian parameterisation is used. The observed signal also agrees with the data from earlier  $e^+e^-$  annihilation experiments, MARKII, CLEO, TPC, TASSO (see references in [23]). The latter results are within the range indicated by the arrows. The comparisons with

---

<sup>2</sup> The default parameter setting does not contain the BE effect

most recent  $\pi^+p$  and  $pp$  data [24] suggest that the BE strength is larger for these two processes. The results from relativistic heavy-ion collisions (not shown) are characterised by significantly larger BE radii, which depend on the atomic number,  $A$ , of the projectile as  $r \simeq 0.7A^{1/3}$  [23].

The BE parameters as functions of  $Q^2$  are shown in Fig. 3. Within errors, the data indicate no variation with the virtuality of the exchanged photon in the range from 0.1 to 5000 GeV<sup>2</sup>. This conclusion is also consistent with the H1 measurement for  $6 < Q^2 < 100$  GeV<sup>2</sup> [4].

## 6.2 Two-Dimensional study

The shape of the correlation function can be studied in more than one dimension after decomposing the momentum difference into the transverse and the longitudinal components. The LEP experiments have recently reported an elongation of the pion source in  $e^-e^+$  annihilation events [25].

Figure 4 shows the BE effect in the transverse and the longitudinal components of momentum difference in the LCMS. Correlations are clearly visible at small  $Q_T$  and  $Q_L$ . The BE correlations in transverse and longitudinal slices are shown in Fig. 5 together with the fit to Eq. (2).

The following values for the correlation function were obtained for  $Q^2 > 110$  GeV<sup>2</sup>:

$$\begin{aligned} r_T &= 0.58 \pm 0.05(\text{stat.})_{-0.12}^{+0.03} (\text{syst.}) \text{ fm}, \\ r_L &= 0.87 \pm 0.06(\text{stat.})_{-0.01}^{+0.09} (\text{syst.}) \text{ fm}, \\ \lambda &= 0.35 \pm 0.03(\text{stat.})_{-0.05}^{+0.03} (\text{syst.}). \end{aligned}$$

The result indicates that the pion-emitting region, as observed in the LCMS, is elongated, with  $r_L$  being larger than  $r_T$ . Assuming a small correlation between radii as for  $e^+e^-$  measurements [25], the obtained ratio is  $r_T/r_L = 0.67 \pm 0.08(\text{stat.})$ , which is consistent with the LEP measurements [25].

The PYTHIA/JETSET implementation of the BE effect does not contain the observed elongation, since the model treats the effect as a final-state interaction by re-shuffling hadron momenta ignoring the directional components of BE. In contrast, the elongation naturally arises in the string fragmentation model [3].

Figure 6 shows the extracted BE parameters as a function of  $Q^2$  for the two-dimensional measurements. No  $Q^2$  dependence of the BE strength is observed, furthermore, the size of the elongation shows no variations with  $Q^2$ .

## 7 Conclusions

One- and two-dimensional Bose-Einstein correlations have been studied in deep inelastic scattering with the ZEUS detector at HERA. The effect was measured as a function of the photon virtuality,  $Q^2$ , in the range from 0.1 to 5000 GeV<sup>2</sup>. Transverse and longitudinal Bose-Einstein correlations have been measured for the first time in DIS. The results indicate that the emitting source of identical pions, as observed in the LCMS, has an elongated shape.

The BE effect in one and two dimensions is observed not to depend on the virtuality of the exchanged photon. The elongation of the pion source is also independent of  $Q^2$ . The observed Bose-Einstein correlations are consistent with the  $e^+e^-$  measurements. This implies that the BE interference is insensitive to details of the hard scattering process.

## References

- [1] G. Goldhaber et al., Phys. Rev. Lett. **3**, 181 (1959);  
G. Goldhaber, S. Goldhaber, W. Lee and A. Pais, Phys. Rev. **120**, 300 (1960).
- [2] B. Anderson and W. Hofmann, Phys. Lett. **B 169**, 364 (1986);  
B. Andersson, Acta Phys. Polon. **B29**, 885 (1998);  
B. Andersson and M. Ringner, Nucl. Phys. **B 513**, 627 (1998).
- [3] B. Andersson and M. Ringner, Phys. Lett. **B 421**, 283 (1998).
- [4] H1 Coll., C. Adloff et al., Z. Phys. **C 75**, 437 (1997).
- [5] G. Goldhaber et al., *Workshop on Local Equilibrium in Strong Interactions*,  
D.K Scott, R.M. Weiner (ed.), p. 115. World Scientific, Singapore, Bad Honnef,  
West Germany (1984).
- [6] T. Csörgó and S. Pratt, *Proceedings of the Budapest Workshop on Relativistic  
Heavy Ion Physics at Present and Future Accelerators*, T. Csörgó et al. (ed.), p. 75.  
(1991). Also in preprint CRIP preprint KFKI-1991-28/A.
- [7] ZEUS Coll., U. Holm (ed.), *The ZEUS Detector*. Status Report (unpublished),  
DESY (1993), available on <http://www-zeus.desy.de/bluebook/bluebook.html>.
- [8] N. Harnew et al., Nucl. Inst. Meth. **A 279**, 290 (1989);  
B. Foster et al., Nucl. Phys. Proc. Suppl. **B 32**, 181 (1993);  
B. Foster et al., Nucl. Inst. Meth. **A 338**, 254 (1994).
- [9] M. Derrick et al., Nucl. Inst. Meth. **A 309**, 77 (1991);  
A. Andresen et al., Nucl. Inst. Meth. **A 309**, 101 (1991);  
A. Caldwell et al., Nucl. Inst. Meth. **A 321**, 356 (1992);  
A. Bernstein et al., Nucl. Inst. Meth. **A 336**, 23 (1993).
- [10] ZEUS Coll., J. Breitweg et al., Phys. Lett. **B 407**, 432 (1997);  
ZEUS Coll., J. Breitweg et al., Phys. Lett. **B 487**, 53 (2000).
- [11] S. Bentvelsen, J. Engelen and P. Kooijman, *Proc. Workshop on Physics at HERA*,  
W. Buchmüller and G. Ingelman (eds.), Vol. 1, p. 23. Hamburg, Germany, DESY  
(1992);  
K.C. Höger. Ibid, p.43.
- [12] F. Jacquet and A. Blondel, *Proceedings of the Study for an ep Facility for Europe*,  
U. Amaldi (ed.), p. 391. Hamburg, Germany (1979). Also in preprint DESY 79/48.
- [13] H. Abramowicz, A. Caldwell and R. Sinkus, Nucl. Inst. Meth. **A 365**, 508 (1995).
- [14] ZEUS Coll., J. Breitweg et al., Eur. Phys. J. **C 12**, 53 (2000).
- [15] L. Lönnblad, Comp. Phys. Comm. **71**, 15 (1992).

- [16] T. Sjöstrand, *Comp. Phys. Comm.* **82**, 74 (1994).
- [17] B. Andersson et al., *Phys. Rep.* **97**, 31 (1983).
- [18] A. Kwiatkowski, H. Spiesberger and H.-J. Möhring, *Comp. Phys. Comm.* **69**, 155 (1992). Also in *Proc. Workshop Physics at HERA*, 1991, DESY, Hamburg.
- [19] H. Spiesberger, *HERACLES and DJANGO: Event Generation for ep Interactions at HERA Including Radiative Processes*, 1998, available on <http://www.desy.de/~hspiesb/djangoh.html>.
- [20] R. Brun et al., *GEANT3*, Technical Report CERN-DD/EE/84-1, CERN, 1987.
- [21] M. Gyulassy, S.K. Kauffmann and L.W. Wilson, *Phys. Rev. C*, 2267 (1979).
- [22] DELPHI Coll., P. Abreu et al., *Phys. Lett. B* **286**, 201 (1992);  
ALEPH Coll., D. Decamp et al., *Z. Phys. C* **54**, 75 (1992);  
L3 Coll., M. Acciarri et al., *Phys. Lett. B* **493**, 233 (2000);  
O. Smirnova, *Nucl. Phys. Proc. Suppl.* **86**, 16 (2000). Proceedings of QCD99, (Montpellier, France, 1999).
- [23] B. Lörstad, *Int. J. Mod. Phys. . A* **4**, 2861 (1989).
- [24] NA22 Coll., N.M. Agababyan et al., *Z. Phys C* **59**, 195 (1993);  
NA 27 Coll., M. Aguilar-Benitez et al., *Z. Phys. C* **54**, 21 (1992).
- [25] L3 Coll., M. Acciarri et al., *Phys. Lett. B* **458**, 517 (1999);  
DELPHI Coll., P. Abreu et al., *Phys. Lett. B* **471**, 460 (2000);  
OPAL Coll., G. Abbiendi et al., *Eur. Phys. J. C* **16**, 185 (2000).

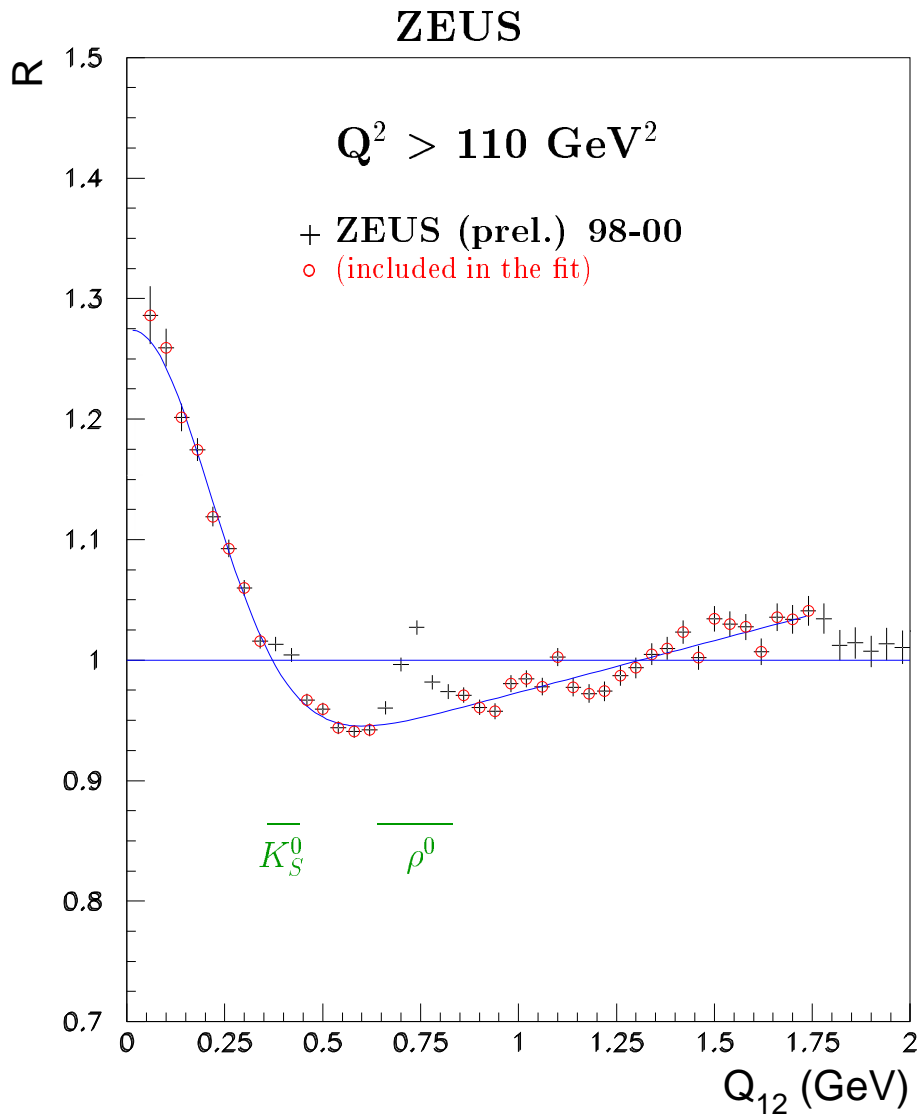


**Figure 1:** *The measured Bose-Einstein correlation function,  $R(Q_{12})$ , together with the fit function from Eq. (1). The error bars show the statistical uncertainties. The data points included in the fit are shown as the circles.*

# ZEUS

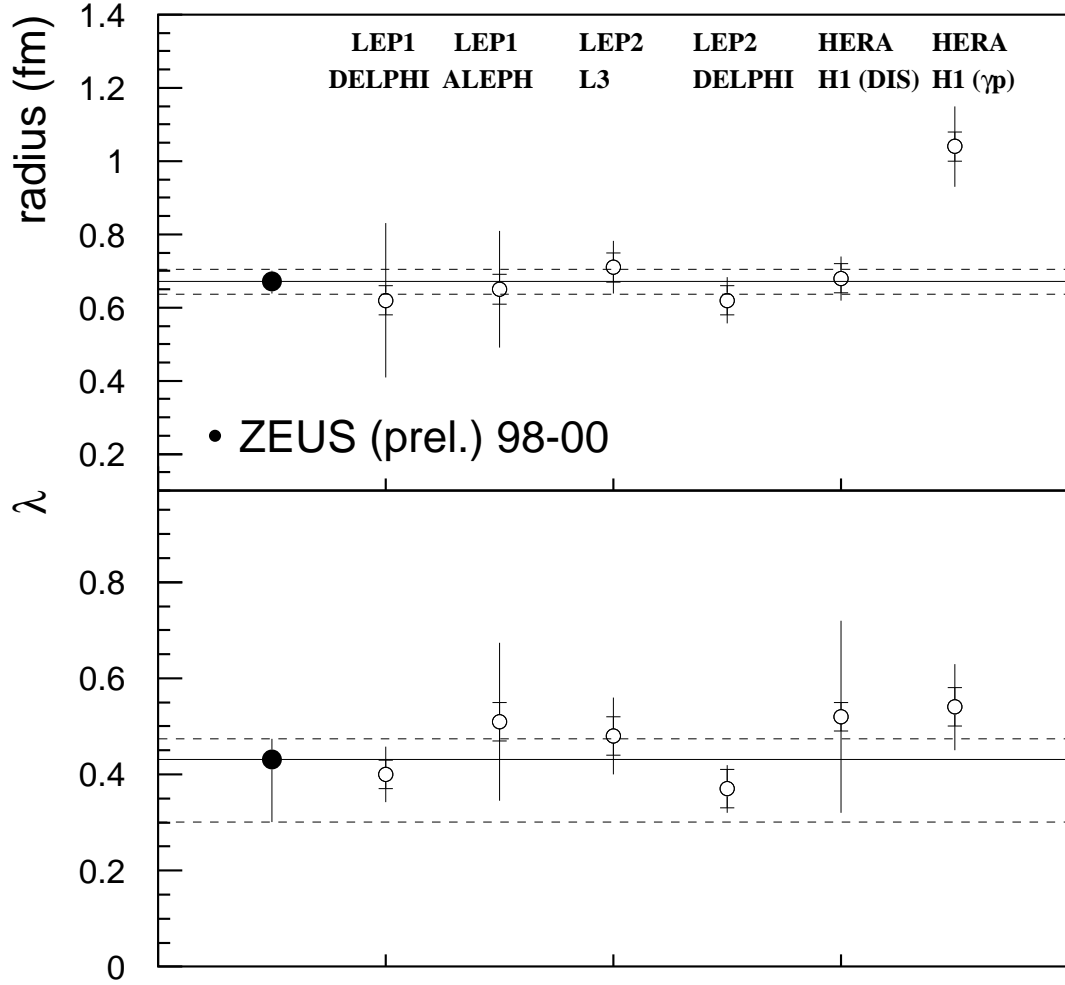


**Figure 2:** Comparison of the measured BE parameters with other experiments. The filled dots show the ZEUS measurements. The inner error bars are statistical uncertainties; the outer are statistical and systematic uncertainties added in quadrature.

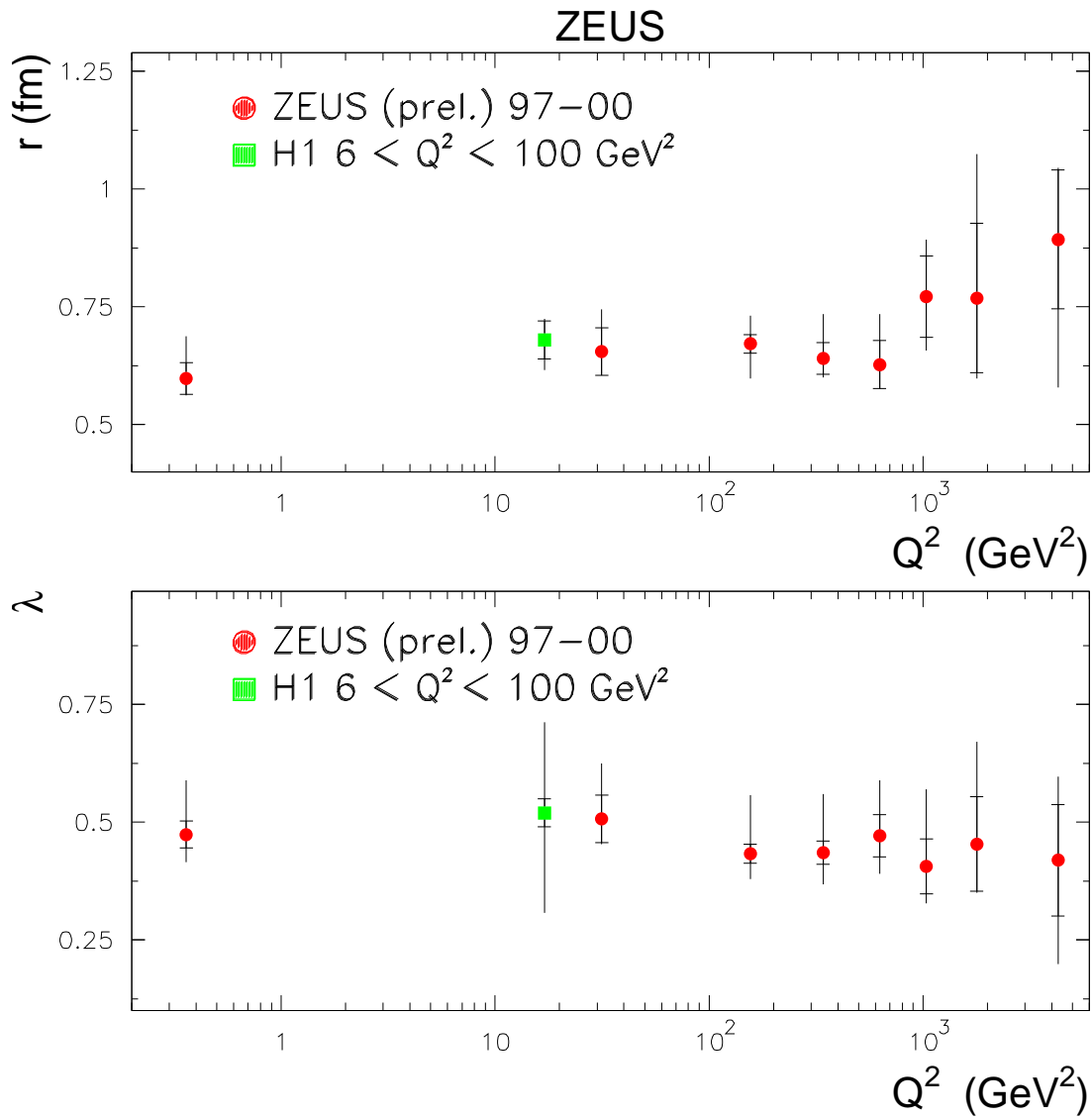


**Figure 3:** *The extracted radius,  $r$ , and the incoherence parameter,  $\lambda$ , as functions of  $Q^2$ .*

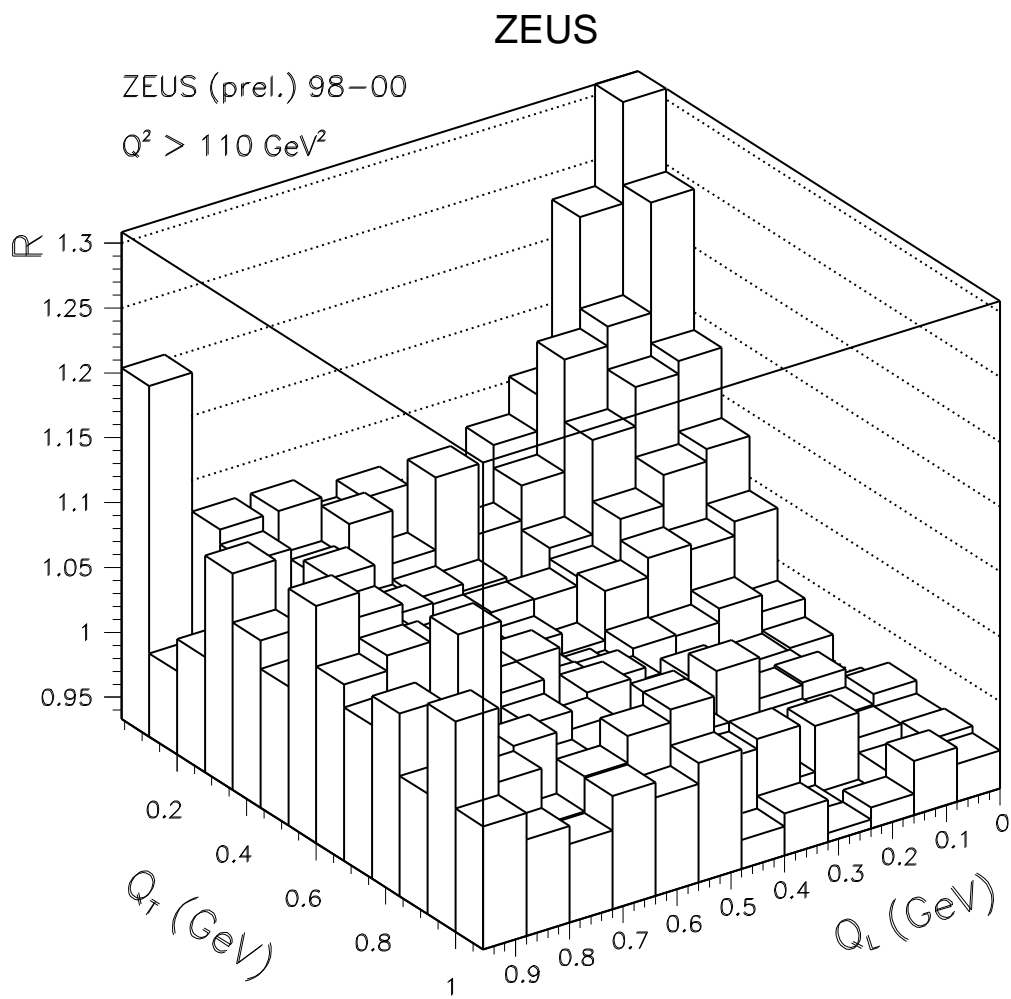


**Figure 4:** *The measured two-dimensional BE function  $R(Q_T, Q_L)$  for  $Q^2 > 110 \text{ GeV}^2$ .*

# ZEUS

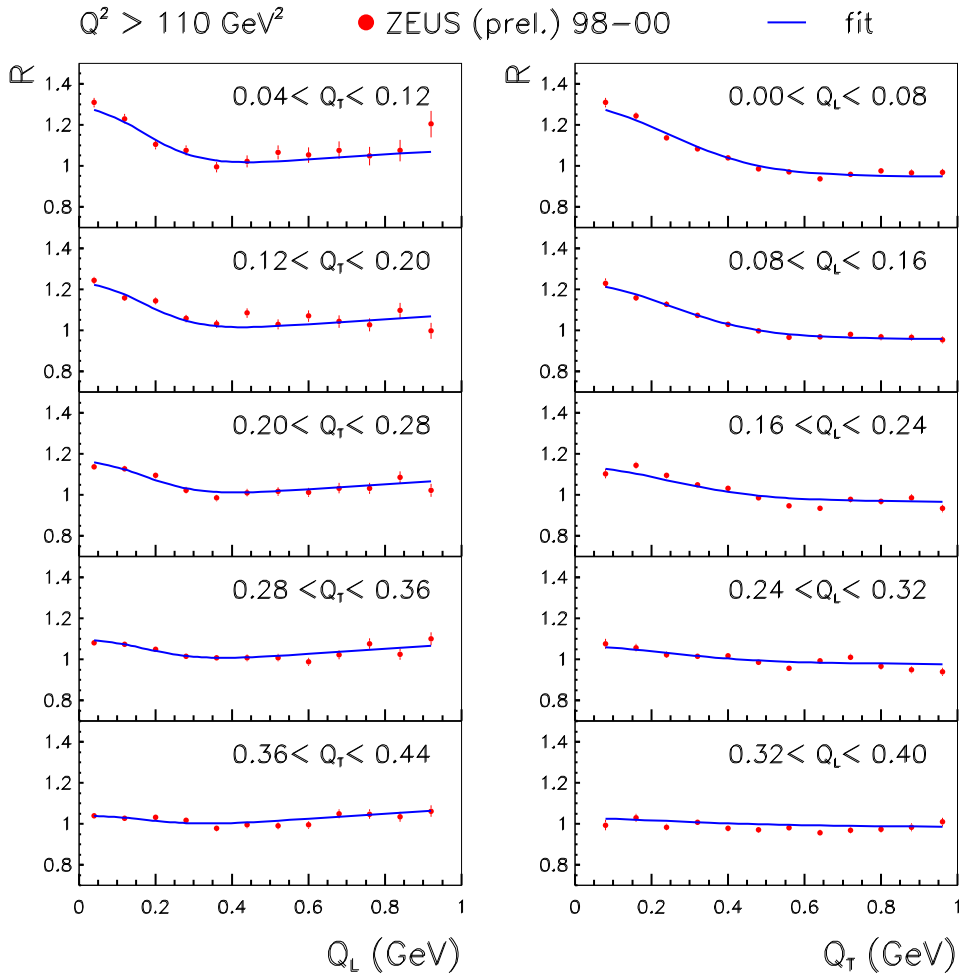


**Figure 5:** *The projections of the two-dimensional BE function  $R(Q_T, Q_L)$  calculated at  $Q^2 > 110 \text{ GeV}^2$ .*

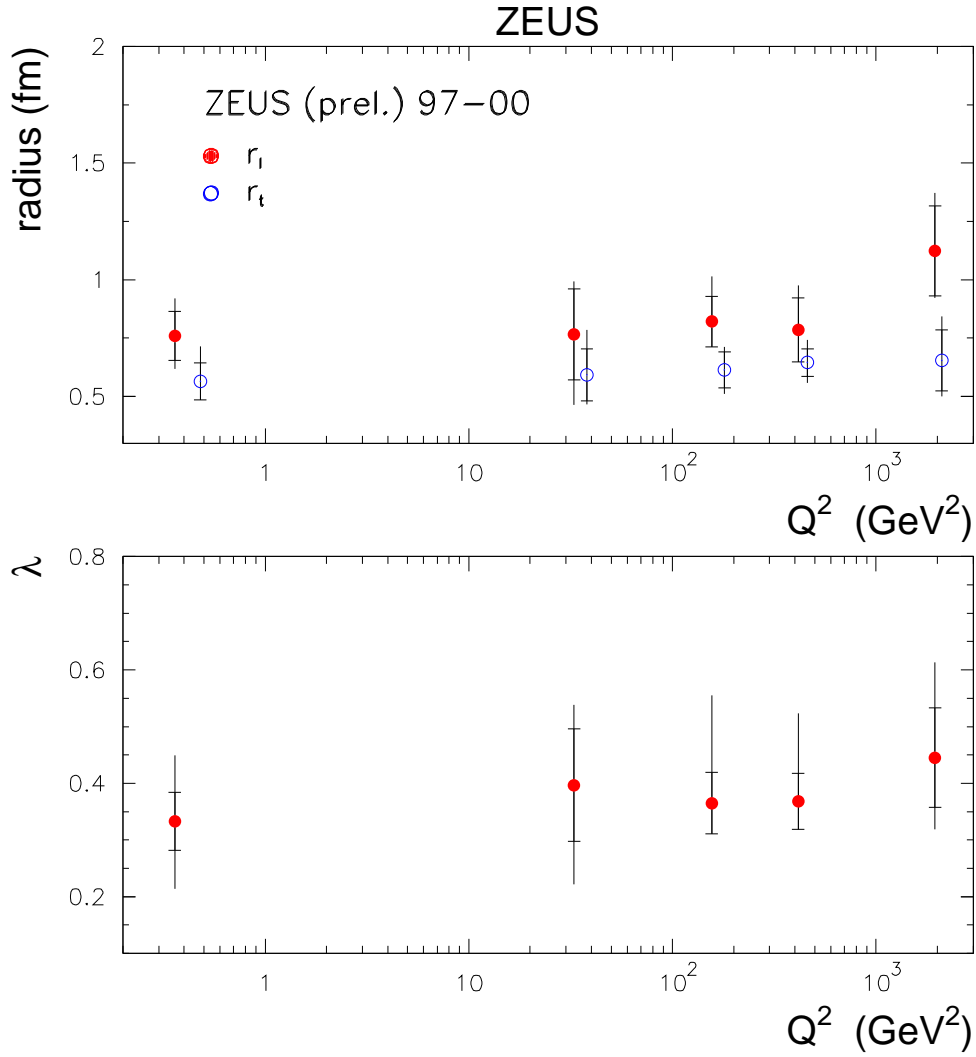


**Figure 6:** The extracted radii, ( $r_t$ ,  $r_l$ ), and the incoherence parameter  $\lambda$  as functions of  $Q^2$  for the two-dimensional correlation function  $R(Q_T, Q_L)$ .